A Finite Element Investigation into the Continuous Induction Welding of Dissimilar Material Joints

Miro Duhovic[1], Joachim Hausmann[1], Pierre L'Eplattenier[2], Inaki Caldichoury[2]

[1]Institut für Verbundwerkstoffe GmbH, Erwin-Schrödinger-Str., Building 58
67663 Kaiserslautern, Germany
[2]Livermore Software Technology Corporation, 7374 Las Positas Road, Livermore,
CA 94551, USA

Abstract

Continuous induction welding is an advanced material processing method with a very high potential of providing a flexible, fast and energy efficient means of joining together thermoplastic composites to themselves and metals and alloys. However, selection of the processing parameters and optimization of the process is very difficult as it involves the interaction of up to four different types of physics. In addition, many different material combinations including materials with low or high electrical conductivity, thermal conductivity and heat capacity, make the intuitive selection of processing parameters impossible. In this work, a simulation test-bed, setup for the continuous induction welding of two material partners and their corresponding physics interactions is used to investigate the induction welding possibilities for several combinations of hybrid material joints. The materials include 2mm thick plates of structural grade aluminium (Al) and steel (St) along with polyamide 6 (PA 6) thermoplastic prepregs containing either glass (GF/PA 6) or carbon fiber (CF/PA 6) reinforcements. In total, six different material combinations are considered (Al-GF/PA 6, Al-CF/PA 6, St-GF/PA 6, St-CF/PA 6, CF/PA 6-GF/ PA 6 and CF/PA 6-CF/PA 6) along with their appropriate weld orientation (i.e. on which side of the material stack the coil should face). A target welding temperature of 250°C is taken for all material combinations as each combination contains the common PA 6 polymer based partner. Surface temperature plots of the developed temperature profile at the coil side surface and welding interface are generated and examined using node selections across the width of the lap-joint at a location where steady state heating has been achieved. Finally, the setup for an ON/OFF switch and proportional-integral-derivative (PID) type process controller is described and initially tested.

1 Introduction

Induction welding is a highly versatile thermoplastic composite (TPC) and hybrid material (metal to composite) fusion bonding process which uses electromagnetic phenomena to generate contact-free heating of the joining partners. The development of a versatile continuous induction welding process has been investigated by various researchers during the last decade [1-5]. In addition, a number of studies have been performed to try and experimentally characterize the heating behavior of various materials using stationary and dynamic heating experiments which investigate the influence of process parameters, such as electromagnetic frequency, generator power, distance between the induction coil and work piece, coil geometry and heat distribution in the work piece [6-13]. One of the main challenges in this case is reliable temperature measurement at the joining interface which is not easy to achieve, as most temperature sensors are affected by the electromagnetic field [14]. Other temperature measurement techniques (e.g. laser pyrometer or infrared camera) only give part of the information, namely temperature information on the surface of the work piece. The temperature measurements help define the correct values of two of the most influential parameters in the process, namely, the 'actual' applied coil current and frequency. The third most influential factor is the temperature and frequency dependent electrical conductivity behavior of the joining materials themselves, however this cannot be controlled. Both sets of data are not easily measured and in addition may change dynamically during the process.

To assist the experimental investigations, numerical simulations have been intensively employed. In this instance, multi-physics finite element models setup in LS-DYNA® mimic experimental setups which consider a heating or induction welding setup and then allow a more complete investigation of the thermal behavior which occurs during the process. This information can then be used to decide on the optimum processing parameters (e.g. the applied coil current or frequency) for various material

combinations which ensure that the material anywhere at the joining interface always remains within its prescribed upper and lower processing temperature limits.

In addition to simulation of the mechanical/thermal/electromagnetic behavior, the capability of LS-DYNA® to also simulate possible types of control systems is also beneficial, as the best control solution can then be implemented in practice. Two typical induction welding control solutions are the basic ON/OFF switch and a PID controller, both of with have been integrated and tested for the first time in the continuous induction welding model presented here.

2 Short overview of continuous induction welding of dissimilar materials

The aims of this work is to setup models in LS-DYNA® which are able to investigate; i) the welding potential of different types of material combinations; ii) obtain an idea of their required processing parameters (e.g. applied coil current) and iii) to examine their resulting thermal behavior during the process. The six different material combinations which have been considered are; carbon fiber (CF) to glass fiber (GF) organosheet, aluminum (AL) to CF/GF organosheet, steel (ST) to CF/GF organosheet and CF to CF organosheet joining via induction welding. As the polymer (PA 6) remains the same in each case, the targeted welding temperature at the joining interface for all cases is fixed at 250°C.

The basic principle of the heating/welding for any of the material combinations can be described as illustrated in Figure 1, which considers the example of an AL/CF joint. Here the induction coil which is connected to a high frequency alternating current source creates a magnetic field within its near surroundings. The alternating magnetic field induces eddy currents in the workpiece (in this case the aluminum) when placed in close proximity to the coil. Heat energy is then generated via the Joule effect as a result of the induced eddy currents flowing through the electrically conductive material. The same can be said if the aluminum is replaced by a steel plate. If the bottom laminate also consists of an electrically conductive material (e.g. CF weave reinforced organosheet) some amount of heating could also be generated in the CF organosheet together with heating resulting from a contact resistance as current is also allowed to flow between the two materials. When the bottom plate consists of a non-electrically conductive material (e.g. GF reinforced organosheet), the heat generated comes only from the metallic partner. Finally, for the two cases where only the composite organosheet is used the required heating effect must come from the CF weave based organosheet. Due to the wide variety of material properties amongst all of these materials, each combination is expected to give very different heating results.

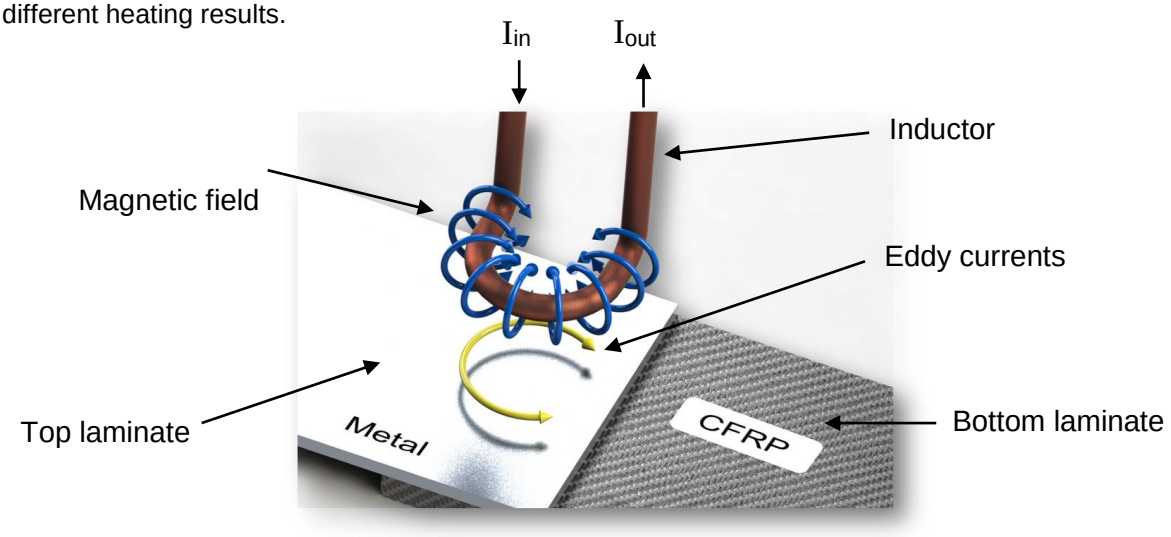

Fig.1: Induction heating principle for hybrid material joints (courtesy of Mrs. Mirja Didi, IVW GmbH)

Upon consideration of the various possibilities concerning the joining partners, one can first consider static single plate heating simulations whereby only the electrical conductivity of the plate is varied. The study is carried out by sampling the maximum temperature developed anywhere in a 0.8 mm thick single plate after 20 seconds of heating using a pancake type coil. The electrical conductivity parameter study has been performed in both LS-DYNA® and COMSOL® and demonstrates the same general results as shown in Figure 2.

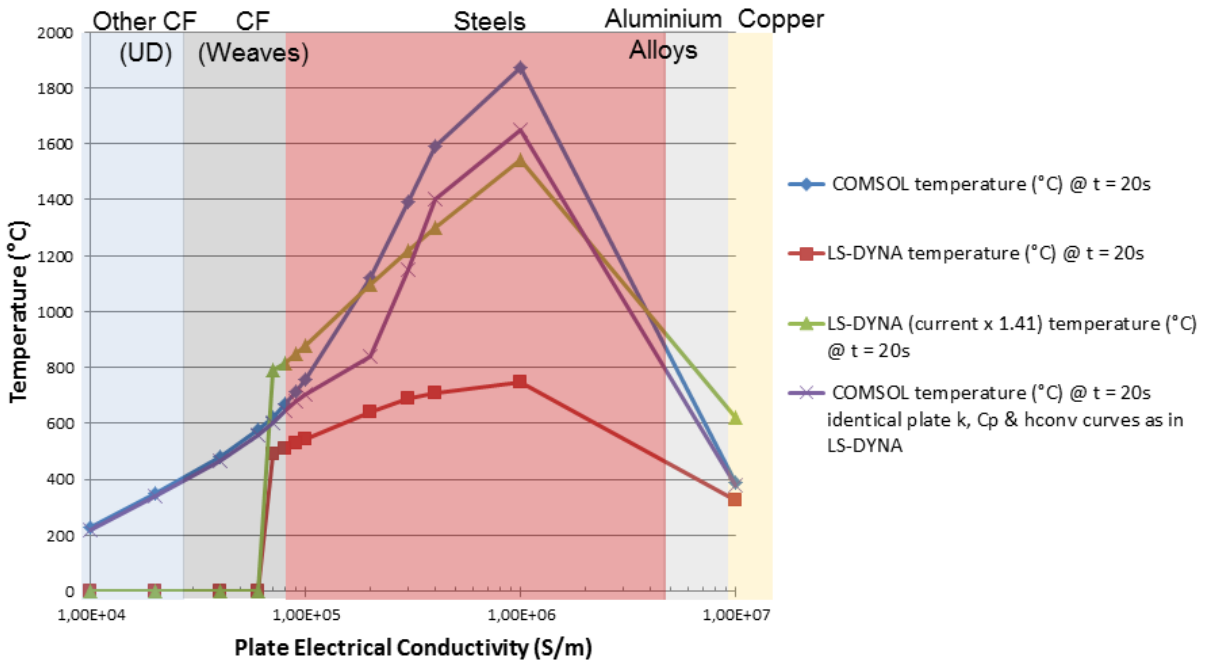

Fig.2: Induction heating effect (maximum temperature developed in 0.8 mm thick plate) in relation to a variation in electrical conductivity

The graph shows an interesting result which suggests that CF weave organosheets whose electrical conductivity (EC) has been measured to be in the order of 10^5 S/m actually produce a better heating effect than aluminum or copper, an observation which has also been seen in practice. The result can be explained by the fact that while a material with a very high EC can support a high current density, the Joule heating losses are very low. In contrast, a material with a very low EC supports a lower current density but the Joule heating losses are very high. Therefore, somewhere in the middle, a peak heating effect exists.

Note that in reality the different materials possess different specific heat capacities as well as thermal conductivities which also influence the result, but nowhere near as much as the applied coil current and the electrical conductivity of the plate being heated [9]. In addition, steel can be a magnetic material and one would also expect to see some heating contribution from magnetic hysteresis, although again, this is much lower than that resulting from eddy current joule losses which can be proven by looking at the nature of the heating pattern. For a pancake coil the magnetic field is most intense at the center of the coil which would result in the most intense heating effect under the center of the coil if only magnetic hysteresis heating was present or was a dominant hearing mechanism which is not the case.

With the above investigation in mind, the orientation (when one has the choice) of the joining partners for welding considered in this study can be logically selected as summarized in Table 1. Combinations 1, 3 and 6 are almost trivial, while 5 and in particular 2 and 4 require a little more thought and are perhaps worth investigating in more detail.

	Mat. Comb. 1	**Mat. Comb. 2**	**Mat. Comb. 3**	**Mat. Comb. 4**	**Mat. Comb. 5**	**Mat. Comb. 6**
Coil side joining partner	CF	CF	AL	CF	GF	CF
Non-Coil side joining partner	GF	AL	GF	ST	ST	CF

Table 1: Orientation selection of material joining partners for continuous induction welding based on EC study

3 Model development of "the induction welding simulative test-bed"

The typical setup for the continuous joining of two composite laminates is illustrated in Figure 3. The graph in the figure presents the typical temperature profile of a fixed point on the top surface of the laminate stack during the induction welding procedure.

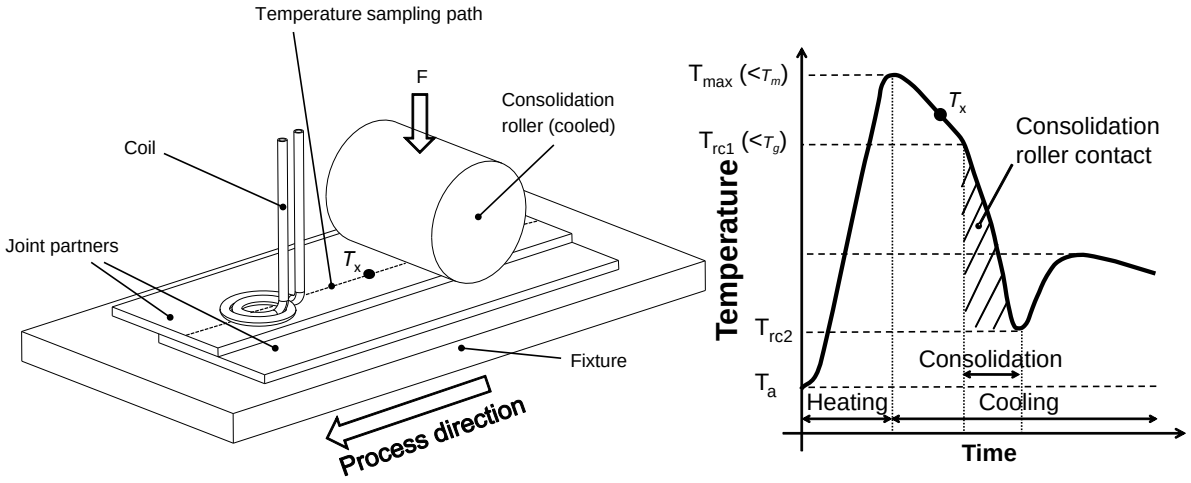

Fig.3: Setup for the continuous induction welding of two composite panels and simplified temperature versus time profile on the top surface of the laminate stack during continuous induction welding (based on data from Rudolf and Moser et al.[2],[9])

As the material passes below the coil, its temperature rises until it reaches T_{max} signifying the end of the heating phase of the process. The temperature then drops slightly due to heat transferred to the jig and surroundings via free convection and conduction until the roller first contacts the measurement point at T_{rc1}. Here the consolidation phase begins and the temperature drops steeply as the roller applies pressure and cools the material to T_{rc2}. Heat inertia resulting from the intrinsic heating then causes a slight rise in the temperature well below melt temperature after which the material then slowly cools to the starting temperature T_a. Note that for ease of explanation, a point on the top surface of the welding stack has been considered. A similar shaped curve, but with less influence from the consolidation roller also exists at the joining interface, whereby T_{max} now, must be less than the degradation temperature of the polymer, T_d (rather than the melt temperature of the polymer, T_m) and T_{rc1} should be equal to or slightly above T_m. T_{rc2} should aim to cool the polymer to below the heat distortion temperature $T_{HDT,}$ where there is no further need for the consolidation roller to apply pressure to the welding stack.

A significant improvement of the continuous welding process was recently achieved by Moser who modified the setup illustrated in Figure 3 by adding an air jet nozzle [9]. The air jet which is applied on the top surface of the laminate stack throughout the heating process essentially alters the through thickness heating gradient so that the highest temperature is achieved at the bond line rather than on the top surface of the laminate. The technique allows the use of higher generator powers and eliminates the problem of excessive heat and thermal degradation on the top surface of the material which is usually the visible surface in a finished part.

All of the necessary features and physics of the continuous induction welding process have been captured in the developed simulation test-bed as shown in Figure 4. The simulation test-bed sets the stage for more complex finite element investigations using moving coil cases where the steady state induction heating temperature patterns become different to that of the static case and are far more difficult to predict and measure. Using this process simulation tool, the effects of the consolidation roller as well as an impinging air jet on the temperature developed on the top surface of the laminate stack, and more importantly the joint interface, can be investigated in full detail. Simulations can be carried out to gain a better understanding of the process and how to go about optimizing it for the dissimilar material combinations specified in Table 1.

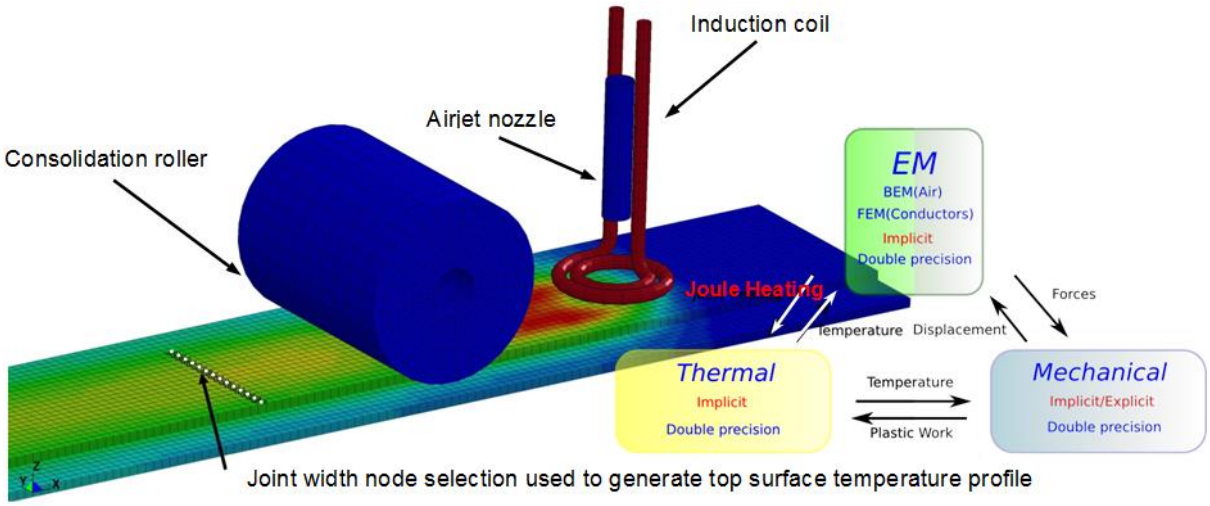

Fig.4: Simulation test-bed setup for the continuous induction welding of two material partners and their corresponding physics interactions developed at the Institut für Verbundwerkstoffe GmbH together with LSTC

3.1 LS-DYNA model structure

The model is setup using a header .dyn file (Figure 5) containing all the input parameters that need to be given in reality in order to carry out actual welding. These inputs are defined via the ***PARAMETER** and ***PARAMETER_EXPRESSION** keywords and are then referenced by their respective parameter symbols within the various keywords in the model. A number of subsystem ***INCLUDE** files are also present which individually reference model data for the induction coil, consolidation roller, cooling nozzle, plate 1, plate 2, and the multi-physical material property data for each material combination. Each of these are grouped into separate ***INCLUDE** files meaning that a simulation can for example be run with or without the cooling nozzle by simply specifying or not specifying it's respective ***INCLUDE** file.

```
*PARAMETER                *INCLUDE                  *INCLUDE
R velocity    3.e-03      $# filename               $# filename
R current     241.54      Aluminium_Roller_60mm.inc Controls.inc
R freq         4.0e5      *INCLUDE                  *INCLUDE
R utemp       523.15       $# filename              $# filename
R ltemp       513.15       Cooling_Nozzle.inc       EM_Controls.inc
*PARAMETER_EXPRESSION      *INCLUDE                  *INCLUDE
R tend    0.3/velocity      $# filename              $# filename
R emdt    tend/100          Plate_1.inc              Material_Combination_CFPA6-CFPA6.inc
*INCLUDE                   *INCLUDE                  *INCLUDE
$# filename                $# filename              $# filename
Pancake_Coil_2mm.inc       Plate_2.inc              Generator_ONOFF_Switch.inc
```

Fig.5: Simulation test-bed model header .dyn file

The model structure therefore allows for different coil coupling distances or even completely different coil, roller and plate geometries to be swapped in and out of the overall model very easily. In Figure 5 it can be seen that for traversing across the 300 mm long welding stack, a velocity of 3 mm/sec, coil current amplitude of 241.54 Amps, frequency of 400 kHz and an upper and lower temperature limit anywhere in the welding zone of 250°C/240°C have been specified respectively. The ***PARAMETER_EXPRESSION** keyword specifies the termination time and EM time step, which both vary according to the selected welding speed. It can be seen that in this way, whatever welding speed is selected, the EM time step is automatically adjusted to keep the overall number of EM time steps and therefore required CPU time constant.

3.2 Physical features of the test-bed model implemented in LS-DYNA®

The simulation test-bed considers all thermal, mechanical and electromagnetic interactions for the case of a two-dimensional induction welding situation as described in Figures 3 and 4. Relative movement between the laminate stack and coil, roller and nozzle has been modelled as in the case of an induction robot welding head performing the operation. Here the coil, consolidation roller and air-jet nozzle are assembled as a unit and are all moved by a robot at constant welding velocities. Mechanical interactions between the consolidation roller plus air-jet pressure and the laminate stack have also been included in the model. This is important since it is a combination of temperature, pressure and time in the correct combination which in the end determines the quality and strength of the joint. The necessary degrees of freedom have been applied to the consolidation roller and a **`*CONTACT_AUTOMATIC_ONE_WAY_SURFACE_TO_SURFACE_SMOOTH_THERMAL`** keyword is used to define the mechanical and thermal contact between the roller and laminate stack which includes static and dynamic friction coefficients enabling an actual rolling contact motion.

A normal force of 300 N, as commonly used in practice, has been applied as the roller traverses the laminate stack. The image inside the plot shows the contours of pressure resulting from roller contact and the air-jet. It can been seen that pressures in the order of 1 MPa are generated as a result of roller contact while those from the air-jet are in reality considerably lower but have been scaled in Figure 6 so that they appear in the plot. In reality, unless very special air-jet nozzles are used, the pressures generated from the air-jet are very low and can be ignored.

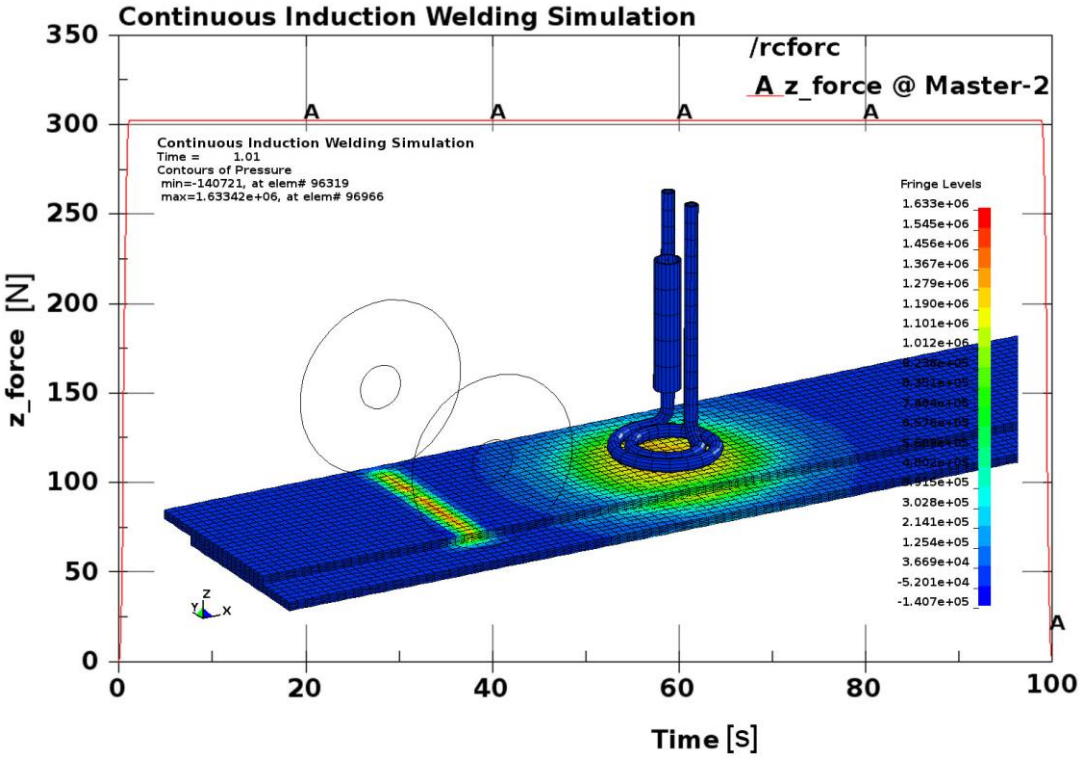

Fig.6: Induction welding simulation test-bed showing the overall roller contact force together with contours of pressure in the laminate generated as a result of roller contact and air-jet pressure

Top surface laminate cooling resulting from the air-jet nozzle blowing air through the center of the pancake coil has been modeled using a "moving heat flux" boundary condition setup via the **`*DEFINE_FUNCTION`** card. An average moving heat flux of 440 W/m^2.K is used which corresponds to a volume flow of an impinging air-jet of 304 liters/min. The moving convection as a function of position is centered on the air-jet nozzle which moves together with the coil and roller and has been assigned an effective cooling area of 80 mm diameter. Roller to laminate contact has been assigned a typical metal to polymer contact heat transfer conductance value of 300 W/m.K.

Although the mechanical interactions are important for calculating overall bond strength they are also required for obtaining the correct thermal behavior. Heat transfer via convection to the surrounding air

and holding fixtures as well as conduction from the laminate stack to the consolidation roller play an important role in determining the overall temperature profile developed in the laminate stack and most importantly at the bond line surface. Details of many of the material properties, thermal and electromagnetic, used in the model can be found in the earlier papers published by Duhovic et al. [6],[7].

To enhance the flexibility of simulating different plate geometries and overlap configurations the "merged nodes" approach used to account for the transfer of mechanical, thermal and electromagnetic contacts has been replaced by considering actual contacts from all three physics. For this the mechanical and thermal contacts are implemented using ***CONTACT_SURFACE_TO_SURFACE_THERMAL** card, while the EM contact is added via ***EM_CONTACT**, ***EM_CONTROL_CONTACT** and the ***EM _CONTACT_RESISTANCE** cards. The exact same simulation using a merged nodes approach takes 93 hrs. versus 119 hrs. (30% more time) for one which considers all the contacts but gives almost identical results using desktop level computing resources (Intel® Core™ i7-4930K 3.40 GHz, 64GB ram and the LS-DYNA SMP solver). Unless considerations of a deforming contact or the contact resistance become greatly important, it is suggested that the models be setup with the contacts, but then that the nodes are merged before running the simulation to reduce the computing time. Figure 7 shows a contour plot of the vector potential showing that continuity between the plates is preserved when all the mechanical/thermal EM contact cards are used.

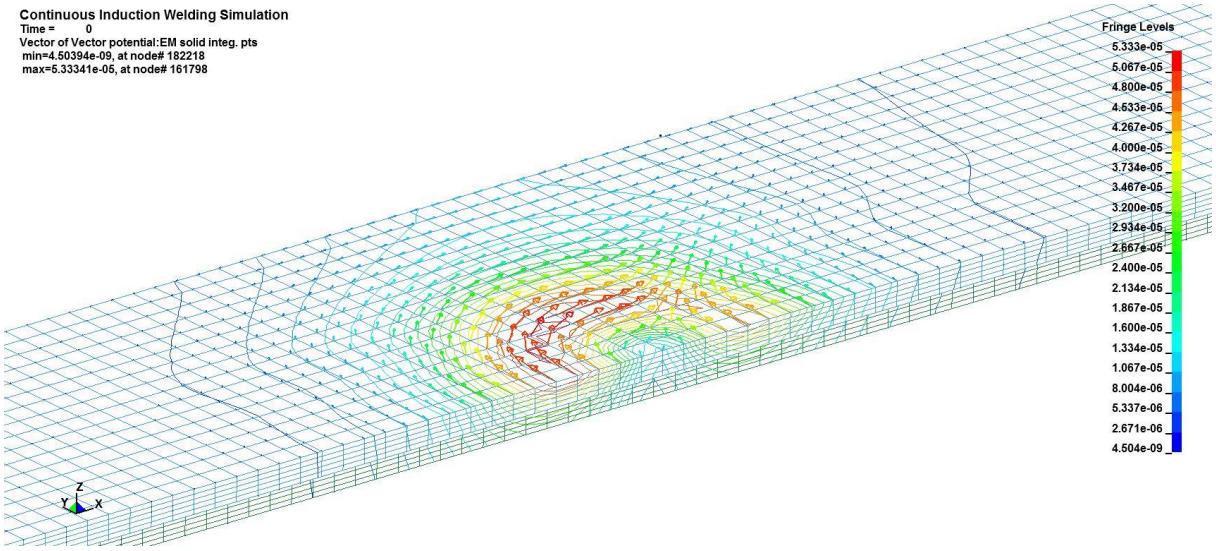

Fig.7: Vector potential continuity between both plates in the welding stack in full contact model

3.3 Implementation of a control system

Two types of control systems have been implemented into the current test-bed model. One is a simple generator ON/OFF switch which is made possible using the keywords ***EM_CONTROL_SWITCH, *DEFINE_CURVE_FUNCTION, *SET_NODE_GENERAL, *SENSOR_DEFINE_NODE_SET, *SENSOR_SWITCH and *SENSOR_CONTROL** cards. Here the upper and lower temperature limits of the welding procedure can be assigned in the ***SENSOR_SWITCH** keyword and are then used together with ***SENSOR_DEFINE_NODE_SET** and the ***SENSOR_CONTROL** cards to send the required integer via the ***DEFINE_CURVE_FUNCTION** to the ***EM_CONTROL_SWITCH** card. The result of the programming is shown in Figure 8, where the maximum temperature anywhere in a CF/PA 6 to CF/PA 6 welding stack is monitored and the EM solver is switched off if only one node anywhere reaches the defined upper limit (523.15K). Likewise the EM solver is switched back on when all of the nodes in the welding stack fall below a specified value (513.15K). Figure 8 also shows the maximum temperature developed in the bond line as a curve. The responsiveness of the switch depends somewhat on the EM and thermal time steps given in to the model which should be small enough to capture the behaviour properly.

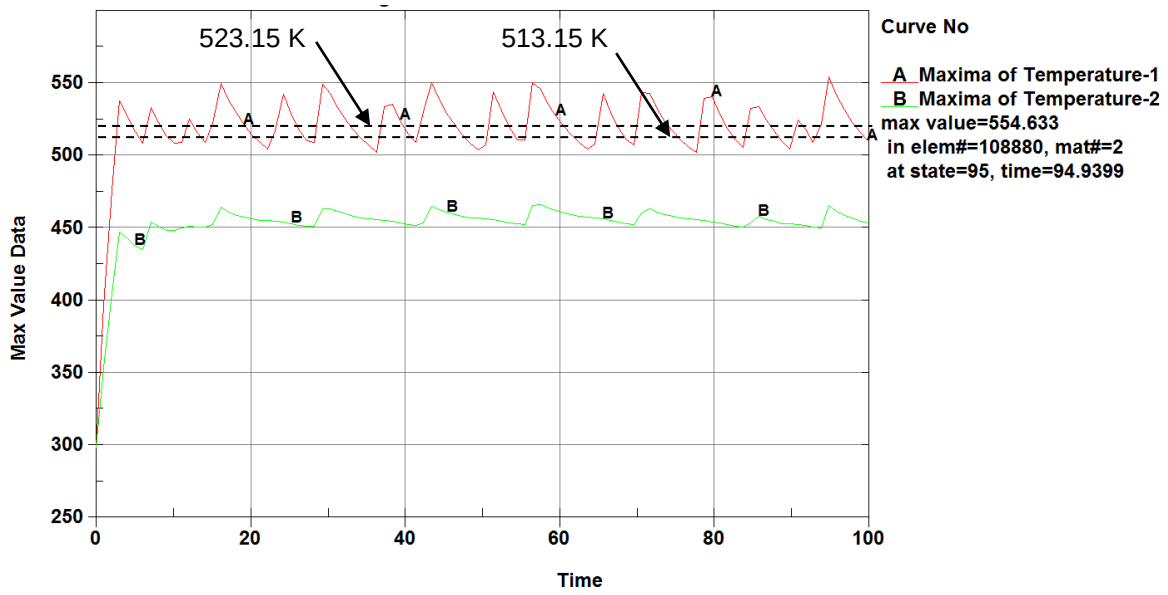

Fig.8: Maximum temperature in the entire welding stack (A) and bond line (B)

A more sophisticated form of process regulation via proportional-integral-derivative (PID) control is also possible. In this case, the keyword ***SENSOR_DEFINE_NODE_SET** is used to monitor the maximum temperature in the welding stack and provide continuous feedback values (temperatures) to ***DEFINE_CURVE_FUNCTION** using the already existing sensor output SENSORD(n) function. The existing PID controller function, PIDCTL(lmeas, ref, lref, kp, lkp, ki, lki, kd, lkd, tf, ltf, ei0, srate, umin, umax), also implemented into a ***DEFINE_CURVE_FUNCTION** and whose parameters can reference the values of other ***DEFINE_CURVE_FUNCTION** can then perform a type of closed loop control. The function is used to regulate the current amplitude defined in the ***EM_CIRCUIT** card by referencing the lcid of the function with a –ve in front of it in place of the usual (+ve) current amplitude value defined. In the future it is hoped that this can be used to find out automatically the correct current amplitude to apply in the case of welding dissimilar material combinations and even to compensate for disturbances when more complex geometries are welded.

4 Initial results of dissimilar material test-bed simulations

Some initial results of the test-bed used to simulate the dissimilar material joints firstly without any control system and then using a PID implementation are presented here. All simulations have been performed using a welding speed of 3 mm/sec and have a coupling distance to the coil side plate (even when this is not electrically conductive, e.g. GF/ PA 6) of 2mm.

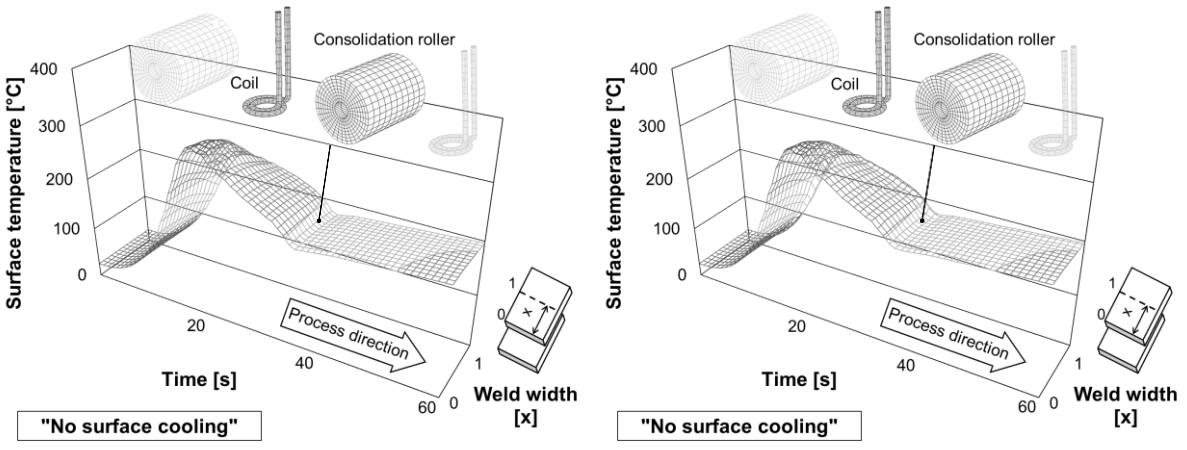

*Fig.9: Surface temperature plots AL/CF **(650A)** for a welding speed 3 mm/sec, fixed coil coupling distance 2 mm and coil to roller offset distance 60 mm; a) top surface and b) joint interface without coil side surface air-jet cooling*

The first example given in Figure 9 shows the top surface temperature and joint interface temperature contours for the material combination of aluminum and carbon fiber PA 6 thermoplastic organosheet (AL/CF). It can be seen that both surface plots look almost identical, indicating that the top surface of the aluminum closest to the coil and the joint interface temperatures are basically the same. It can also be seen that an equal temperature distribution across the width of the weld is achieved even though the coil geometry itself produces a non-uniform heating pattern. The very high thermal conductivity of aluminum is believed to be the key factor for this. The cooling effect of the consolidation roller can be seen only slightly in both of the temperature contour plots as the steepest dip in the cooling curve and as indicated in Figure 9.

The second combination demonstrated is that of carbon fiber PA 6 thermoplastic organosheet induction welded to itself. In this case, it can be seen that the poor thermal conductivity of the composite results in a very uneven temperature distribution across the width of the weld. This is strongly visible on the top surface laminate closest to the coil, but also at the joint interface as shown in Figure 10. This can be problematic for the welding of such materials as the temperature processing range required to create a weld across the entire weld width can be too large. The highest peaks in the curves which generate the surface plot should therefore lie between the melt and degradation temperature of the polymer if a full weld across the entire width is to be achieved.

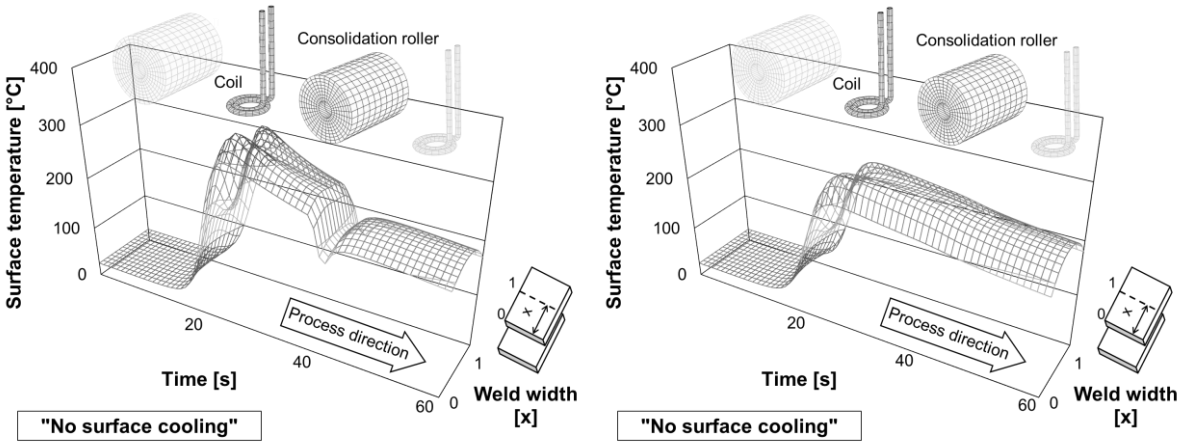

a) **b)**

*Fig.10: Surface temperature plots CF/CF **(195A)** for a welding speed 3 mm/sec, fixed coil coupling distance 2 mm and coil to roller offset distance 60 mm; a) top surface and b) joint interface without coil side surface air-jet cooling*

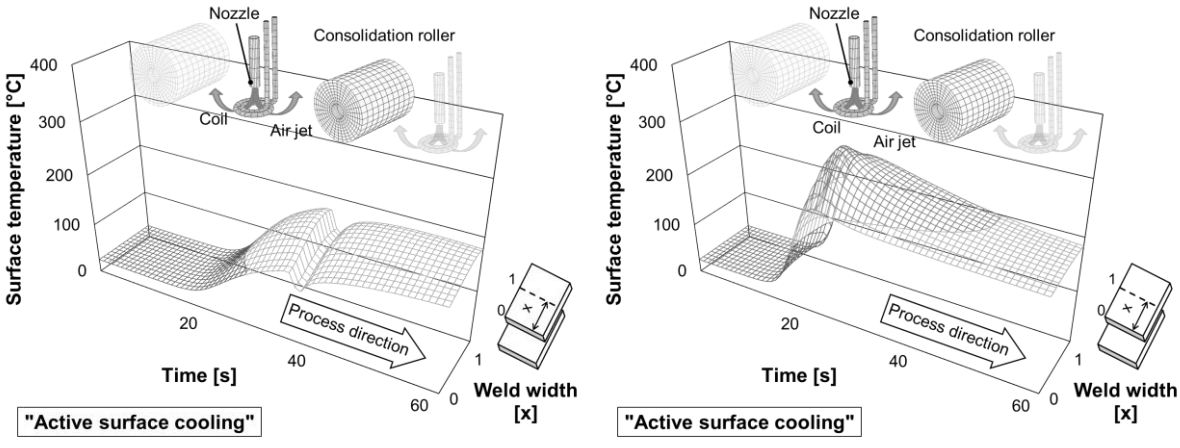

a) **b)**

*Fig.11: Surface temperature plots GF/ST **(270A)** for a welding speed 3 mm/sec, fixed coil coupling distance 2 mm and coil to roller offset distance 60 mm; a) top surface and b) joint interface with coil side surface air-jet cooling*

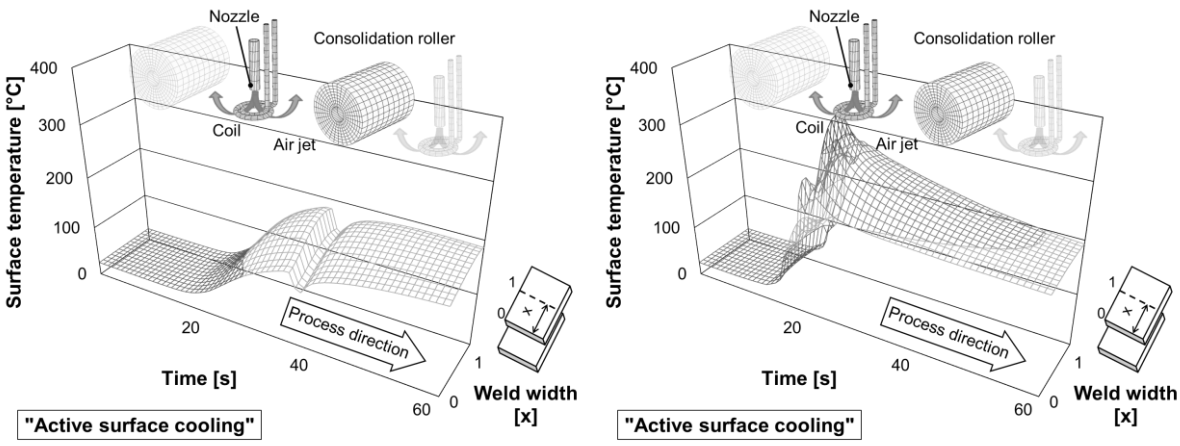

*Fig.12: Surface temperature plots GF/ST **(PID Control with 300°C as set point)** for a welding speed 3 mm/sec, fixed coil coupling distance 2 mm and coil to roller offset distance 60 mm; a) top surface and b) joint interface with coil side surface air-jet cooling*

Figures 11 and 12 both show the case of a non-conductive thermoplastic organosheet material induction welded to steel (GF/ST). An air jet cools the top surface of the organosheet as it removes heat from the steel plate. With no control system and a fixed coil current of 270A, a relatively uniform temperature distribution compared to the case where PID control is used can be seen. In this case, the PID controller seems to fluctuate between the “umin” and “umax” parameters defined in the controller function in order to achieve the desired maximum temperature set point of 300°C resulting in a switch type behavior. Further work in tuning the PID controller parameters for the test-bed model is required with the aim of obtaining a smooth rise to the desired set point temperature by manipulating the coil current.

5 Summary

The current work has described the setup in LS-DYNA® of a simulation test-bed for the finite element investigation of continuously induction welded dissimilar material joints. Firstly, a parameter study regarding the Joule heating effect in induction heated plates of varying electrical conductivity was performed to reveal the necessary coil current and therefore generator power levels required to inductively heat and therefore weld different material combinations. It was shown that although thermoplastic composites containing carbon fiber weave reinforcement have a very low electrical conductivity, the heating effect is much higher than in that of aluminum. The LS-DYNA® model structure of the continuous induction welding simulation test-bed was then described in detail and the functionality of the model was presented. Surface temperature plots for some selected material combinations were presented and discussed emphasizing the difference in the temperature profile across the width of the weld for the given coil geometry. Furthermore, two options for including process control into the model, namely temperature based ON/OFF switch type control and PID control were implemented into the test-bed model. It was apparent that an ON/OFF switch type control is not sufficient for the process. A smooth regulation of the coil current via PID control will be implemented in the future by correctly tuning the necessary function parameters. It is then expected that the coil current is automatically adjusted by the PID controller given the properties of the material combination to be welded and the desired welding temperature which can be specified in the model by the user.

6 Acknowledgments

The authors would like to thank Mr. Arthur Shapiro for the keyword function code which defines the cooling air-jet moving convection boundary condition and also Mr. Isheng Yeh for the implementation of the sensor keyword options allowing the detection of max temperature in a part for implementation together with the PID controller capability.

7 Literature

[1] Zach T, Lew J, North TH, Woodhams RT. Joining of high strength oriented polypropylene using electromagnetic induction bonding and ultrasonic welding. Mat Sci Tech 1989; 5: 281-287.

[2] Rudolf R, Mitschang P, Neitzel M: Induction heating of continuous carbon-fibre-reinforced thermoplastics. Composites Part A 2000; 31: 1191–1202.

[3] Shevchenko N, Fink BK, Yarlagadda S, Tierney JT, Heider D, Gillespie JW Jr. Rapid Automated Induction Lamination (RAIL) for High-Volume Production of Carbon/Thermoplastic Laminates. ARL-TR-2478. Aberdeen Proving Ground: Army Research Laboratory, 2001.

[4] van Wijngaarden MJ. Robotic induction welding of carbon fiber reinforced thermoplastics. In: SAMPE Fall Technical Conference, Seattle, 2005, code 68836.

[5] Mitschang P, Velthuis R, Emrich S, Kopnarski M. Induction Heated Joining of Aluminum and Carbon Fibre Reinforced Nylon 66. J Therm Comp Mat 2009; 22: 767-801.

[6] Duhovic M, Moser L, Mitschang P, Maier M, Caldichoury I, L'Eplattenier P: Simulating the Joining of Composite Materials by Electromagnetic Induction. In: Proceedings of the 12th International LS-DYNA® Users Conference, Detroit, 2012, Electromagnetic (2).

[7] Duhovic M, Caldichoury I, L'Eplattenier P, Mitschang P, Maier M. Advances in Simulating the Joining of Composite Materials by Electromagnetic Induction. In: Proceedings of the 9th European LS-DYNA® Users Conference, Manchester, 2013, Electromagnetic (2).

[8] Duhovic M, Hümbert M, Mitschang P, Maier M, L'Eplattenier P, Caldichoury I,. Further Advances in Simulating the Processing of Composite Materials by Electromagnetic Induction. In: Proceedings of the 13th International LS-DYNA® Users Conference, Detroit, 2014, Electromagnetic

[9] Moser L. Experimental Analysis and Modelling of Susceptorless Induction Welding of High Performance Thermoplastic Polymer Composites. Kaiserslautern: IVW GmbH, 2012.

[10] P. Mitschang, R. Velthuis and M. Didi, "Induction Spot Welding of Metal/CFRPC Hybrid Joints", Adv. Eng. Mater., 2013.

[11] P. Mitschang, R. Velthuis, S. Emrich, M. Kopnarski, "Induction Heated Joining of Aluminum and Carbon Fibre Reinforced Nylon 66". J Therm Comp Mat 2009; 22: 767-801.

[12] S. Schmeer, F. Balle, M. Didi, G. Wagner, M. Maier, P. Mitschang, and D. Eifler, "Experimental and simulational characterization of spot welded hybrid Al/CFRP-joints on coupon level", Adv. Eng. Mater., 2013.

[13] S. Schmeer, F. Balle, M. Didi, S. Huxhold, G. Wagner, P. Mitschang, M. Maier, and D. Eifler, "Experimental and computational analysis of multi-spot welded hybrid Al/CFRP-structures on component level", Adv. Eng. Mater., 2013.

[14] Schieler O, Beier U, Mitschang P. Temperature measurement in electromagnetic fields – by the example of the induction welding process. Journal of Thermoplastic Composite Materials, 2014.